# Manifestations of induced molecular alignment in the interaction of ultrafast laser pulses with gases

**A A Kolomenskii[1], N Kaya[2,3], G Kaya[2], M Sayrac[1], Y Boran[1], J Strohaber[4] and H A Schuessler[1,2]**

[1]Department of Physics and Astronomy, Texas A&M University, College Station, Texas 77843-4242, USA.
[2]Science Program, Texas A&M University at Qatar, Doha 23874, Qatar.
[3]Department of Physics, Giresun University, Giresun 28200, Turkey.
[4]Department of Physics, Florida A&M University, Tallahassee, Florida 32307, USA.

**Abstract.** The dynamics of rotational wave packets of laser-aligned linear molecules was studied with femtosecond laser pulses in a pump-probe configuration. The alignment produced with a pump beam creates a transiently anisotropic medium, which exhibits birefringence and also a dependence of ionization on the mutual orientation of the polarizations of the probe and pump beams. The induced molecular alignment was observed via variations of the yields of photoelectrons in strong field ionization. In addition, the induced transient birefringence due to alignment revivals altered the nonlinear interaction of the probe beam with the gas, resulting in delay dependent modulation of the probe beam. The revival signatures measured for $N_2$, CO and $C_2H_2$ gas molecules were in good agreement with the calculated molecular alignments taking into account the effects of electronic structure and molecular symmetry.

## 1. Introduction

In the nonadiabatic alignment, i.e. when the laser pulse duration is less than the characteristic molecular rotational period, the short laser pulse induces in molecules a rotational wave packet. The dipole moment due to the anisotropic polarizability of the molecule tends to align its axis of highest polarizability along the laser polarization direction [1]. The produced wave packet, i.e. a coherent superposition of the rotational states shows dephasing and re-phasing in time after the laser pulse has ended. Consequently, the gaseous medium exhibits anisotropic properties, which depend on the delay relative to the excitation pump pulse. Studies on molecular alignment and orientation in molecules (see [2, 3]) have attracted considerable interest due to the variety of applications and different manifestations of the alignment process, such as controlling chemical reactions [4], selectively-controlled alignment of isotopes [5], imaging of molecular structures [6], nanolithography with molecular beams [7], pulse compression [8], and quantum information processing [9]. Femtosecond laser technology allows aligning molecules and observing the molecular dynamics by using a pump-probe technique [10]. Alignment initiated by a pump pulse creates a dynamically anisotropic medium evolving in time, and hence, concurrent variations of the interaction with such a medium of a probe pulse can be observed by ionization [11], fragmentation [12, 13], high harmonic generation [14] or by spatial and spectral modulation of the probe pulse [15-17].

For many applications, it is important to align molecules outside the plane of polarization [18], which can be achieved by circularly polarized probe pulses. The circularly polarized aligning pulse produces a torque on the molecules by pulling the most polarizable axis into the plane of polarization. This creates

a rotational wavepacket that re-aligns under field-free conditions to the plane of polarization every revival period [2]. For a linear molecule, just before the revival, the molecular axis first aligns along the direction of laser propagation, which is called 'k-alignment' [19], then the molecule keeps rotating, and in a short time later the molecular axis is aligned with the field polarization plane.

Of particular interest is the effect of alignment on filament formation and white light generation. The nonlinear polarization exerted by a pump pulse yields an intensity-dependent refractive index and a transient birefringence as a result of the pulse interaction with the molecular gas. Then a probe pulse propagates in a medium with properties that depend on the delay in the wake of the pump pulse. For certain conditions, the intense probe pulse can experience self-focusing and spatially collapses due to the dynamic Kerr effect. This collapse however stops when the intensity becomes high enough to generate free electrons and nonlinear losses tending to defocus the beam resulting in filamentary propagation [20]. The spatial and temporal characteristics of the aligned molecules affect filamentation and white light generation [21], so these processes can be also used for probing the dynamics of molecular alignment. Here we present our recent work on different manifestations of molecular alignment in the interaction of intense femtosecond laser pulses with molecular gases. We monitored the effect of aligning by observing the strong field ionization yield of photoelectrons by using a pump-probe approach. The molecular ionization rate is often maximal when the maximum of the initial electron density distribution corresponds to the laser polarization direction of the applied field. However, not all diatomic molecules have their highest occupied molecular orbital (HOMO), which donates electrons most readily, aligned along the molecular axis. The measured molecular alignment is compared to the calculated time dependence of the molecular alignment parameter $\left\langle\left\langle \cos^2\theta \right\rangle\right\rangle$, and the effects of the electronic structure and symmetry of molecules on the signatures of alignment revivals were investigated. We study effects of molecular alignment with linear and circularly polarized laser pulses on strong field photoionization of electrons. We also observed transmission spectral modulation of a probe pulse due to the induced transient birefringence produced by alignment revivals. By changing the angle between polarizations of the pump pulse and the filament-producing probe pulse and performing measurements for a range of pump-probe delays around rotational revivals, we obtained a map of the rotational wave packet as a function of the polarization mismatch and the delay between the pump and probe pulses, which is also known as a "quantum carpet" [22]. The experimental results on the dynamics of rotational wave packets are compared with quantum-mechanically calculated angular and time dependencies of the molecular alignment parameter, showing good agreement.

## 2. Theory

The time-dependent Schrödinger equation describing a molecule in an intense laser field can be written based on the rigid rotor model as

$$i\hbar\frac{\partial}{\partial t}\Phi_{JM}(t)=\left(H_R^{(0)}+V_L(t)\right)\Phi_{JM}(t), \tag{1}$$

where $H_R^{(0)}=B\hat{J}^2$ is the field-free rotational Hamiltonian of the molecule with $B$ and $\hat{J}$ being the rotational constant and the angular momentum operator, respectively. The interaction term is $V_L(t)=-\frac{1}{2}\,\Delta\alpha\cos^2\theta+\alpha_\perp\,\left\langle\varepsilon^2\ t\right\rangle$ for a linear symmetric top molecule subjected to the linearly polarized laser field $\varepsilon\ t$ of the field of the pump pulse; in case of a circular polarization the expression of the nonresonant dipole potential for circular polarization becomes $V\ t=-1/4\ \alpha_\parallel+\alpha_\perp-\Delta\alpha\cos^2\theta\ E^2\ t$ [23-26], where $\Delta\alpha=\alpha_\parallel-\alpha_\perp$ is the difference between the polarizability components parallel $\alpha_\parallel$ and perpendicular $\alpha_\perp$ to the molecular axis and $\theta$ is the angle between the molecular axis and the field propagation direction of the aligning pulse.

The rotational wave function $\Phi\ t$ can be expanded in a sum of free-field rotor eigenfunctions $\left|JM\right\rangle$ with eigenenergies $E_J = BJ\ J+1$ , where $J$ is an integer of the orbital momentum quantum number, and for each $J$ the projection quantum number $M$ takes the values $-J$ , $-(J-1)$, ..., 0, ...$(J-1)$, $J$ . Then the evolution of the initial state, $\left|\Phi_{J_0M_0}(t)\right\rangle$, created by the pump pulse is described by an expansion in the rotational wave packet states [2]:

$$\left|\Phi_{J_0M_0}\ t\ \right\rangle = \sum_{JM} d_{JM}^{J_0M_0}\ t\ \exp\left(-i\frac{E_J}{\hbar}t\right)\left|JM\right\rangle, \tag{2}$$

where the expansion coefficients $d_{JM}^{J_0M_0}\ t$ are determined by solving the set of differential equations [27] stemming from the time-dependent Schrödinger Eq. (1). The degree of alignment of an ensemble at temperature *T* can be found by averaging the different states over the Boltzmann distribution

$$\left\langle\left\langle\cos^2\theta\right\rangle\right\rangle\ \mathbf{r},t\ = \frac{\sum_{J_0}\sum_{M_0=-J_0}^{J_0} g_{J_0}\left\langle\cos^2\theta\right\rangle_{J_0M_0}\ \mathbf{r},t\ \exp\ -BJ_0\ \ J_0+1\ /kT}{\sum_{J_0}\sum_{M_0=-J_0}^{J_0} g_{J_0}\exp\ -BJ_0\ \ J_0+1\ /kT}\ , \tag{3}$$

where $\left\langle\cos^2\theta\right\rangle_{J_0M_0}\ \mathbf{r},t\ = \left\langle\Phi_{J_0M_0}\ t\ \right|\cos^2\theta\left|\Phi_{J_0M_0}\ t\ \right\rangle = \sum_{J',M'}\sum_{J,M} d_{J'M'}^{*J_0M_0} d_{JM}^{J_0M_0}\left\langle J',M'\right|\cos^2\theta\left|J,M\right\rangle\varphi_{J,J'}$ is the alignment degree for a single individual rotational state $\left|J_0M_0\right\rangle$, $\varphi'_{J,J\pm2} = \exp\left[-\mathrm{i}\ \pi\tau(4J+6)+\Delta\ \right]$ , where $\Delta$ is determined by the configuration of the HOMO orbital. We note that $\left\langle\cos^2\theta\right\rangle_{J_0M_0}\ t$ depends on coefficients $d_{JM}^{J_0M_0}\ t$ , which in turn are determined by the interaction term that has certain spatial distribution over position vector $\mathbf{r}$ . An additional factor $g_{J_0}$ originates from the nuclear spin statistics. The alignment degree depends on molecular properties, i.e., the rotational constant *B*, statistical weight factors $g_{J_0}$, the ensemble temperature *T* and the polarizabilities $\Delta\alpha$ as well as on the laser fluence.

When molecules with anisotropic polarizability experience the aligning (pump) pulse in a non-adiabatic alignment regime, the refractive index changes both spatially and temporally. The nonadiabatic molecular alignment induces a periodic modulation of the refractive index $\Delta n\ \mathbf{r},t$ of the gas. For the probe pulse with the polarization direction of the aligning pulse the resulting birefringence can be characterized by the difference [28]

$$\Delta n\ \mathbf{r},t\ = \Delta n_{\parallel}\ \mathbf{r},t\ - \Delta n_{\perp}\ \mathbf{r},t\ = \frac{3\pi N}{n_0}\Delta\alpha\left(\left\langle\left\langle\cos^2\theta\right\rangle\right\rangle\ \mathbf{r},t\ -\frac{1}{3}\right), \tag{4}$$

where $\left\langle\left\langle\cos^2\theta\right\rangle\right\rangle\ \mathbf{r},t$ is the thermally averaged alignment expectation value given by Eq. (3), *N* is the molecular density, and $n_0$ is the linear refractive index. The spatial dependence, which follows the intensity distribution of the pump beam, creates an additional lensing effect for the probe beam due to the spatially inhomogeneous molecular alignment. We note that polarizabilities are modified when the field becomes sufficiently strong, in particular, absorption can include also the contribution from multiphoton processes and the changes of both the real and imaginary parts of the refractive index are proportional to the alignment factor, $\left(\left\langle\left\langle\cos^2\theta\right\rangle\right\rangle(\mathbf{r},t)-\frac{1}{3}\right)$.

## 3. Experimental setup

The pump-probe setup is depicted in Figure 1. A mode-locked Ti:sapphire laser oscillator provides ~20fs pulses at a repetition rate of 80 MHz. These pulses are seeded into a regenerative laser amplifier, which

outputs ~50fs laser pulses at a repetition rate of 1 kHz and a central wavelength of 800 nm. Since shorter pulses have a higher peak intensity for a given pulse energy, temporal compression of the laser pulses in the focus was achieved by maximizing the integrated photoelectron yield, while adjusting the grating compressor in the laser amplifier. The maximum pulse energy from the amplified laser system was ~1 mJ.

In the experiments, different gases ($N_2$, CO or $C_2H_2$ from Matheson TRIGAS, with purities of 99.9995%, 99.9%, 99.6%, respectively) were admitted to the chamber through an adjustable leak valve. The pressure of the gases in the chamber was adjusted to $6\times10^{-6}$ mbar, which was about three orders of magnitude higher than the background pressure. The linearly polarized incident light was split by a beam-splitter into two beams as pump and probe pulses with about equal intensities. A set consisting of a half-wave plate and a polarizer was placed into the pump arm assuring the proper polarization and intensity of the pump pulse.

The time delay between the pump and probe pulses was precisely adjusted using an optical delay line with a translational stage controlled by a stepping motor (GTS150, ESP300, Newport), which provided a high temporal resolution of ~0.67 fs. Another beam-splitter was used to recombine the two beams. The laser beam was focused in the chamber filled with gas by a 20cm achromatic lens. The pump pulse creates a rotational wave packet, while the probe pulse, with an adjustable time delay with respect to the pump pulse, ionizes molecules in the focus, producing electrons. The ionized electrons, ejected along the polarization direction of the probe laser field were detected by the MCP detectors. The electrons traveled within a μ-metal TOF tube in a magnetic field-free region. The signals from the MCP detectors were amplified by a preamplifier (ZKL-2 Mini-Circuits). A FAST ComTech MCS6 multiple-event time digitizer with 100 ps time resolution was used for data acquisition. Laser pulses were detected behind one of the mirrors on the probe arm by a photodiode, and the signal was used to trigger the data-acquisition software. The total number of counts, depending on the pump-probe delay, was registered as the output signal.

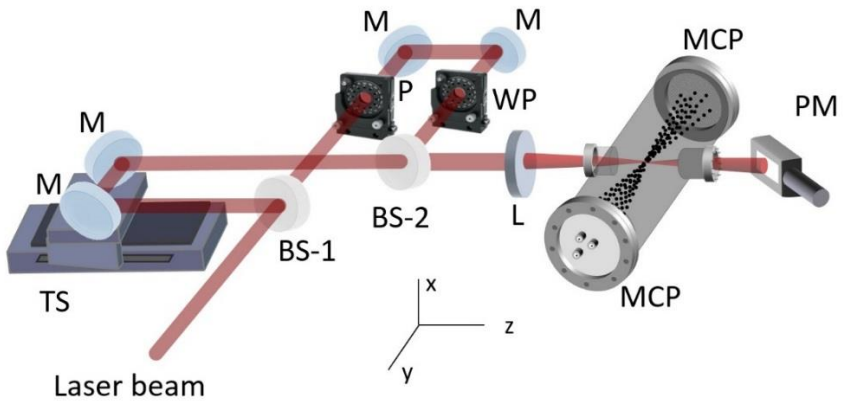


**Figure 1.** Experimental setup. BS: beam-splitters, TS: translational stage, WP: wave plate, M: flat mirrors, L: achromatic focusing lens, PM: power meter, MCP: microchannel plates. The dots depict electrons flying toward the MCP detectors.

When studying induced gas birefringence we used a gas cell at relatively high pressure (~4bar) instead of the vacuum chamber utilized in experiments with photoelectrons. In addition, the power measurement of the probe pulse variations were performed by using a photodiode power meter (Ophir NOVA II with PD300-UV head), the spectral measurements were performed with an Ocean Optics USB-2000 spectrometer and the pulse duration measurements were done with a correlator Grenouille (8-20, Swamp Optics).

## 4. Linear molecules aligned with linearly polarized laser pulses

We have observed alignment effects [29] with different gases: $N_2$, CO, and $C_2H_2$. The choice of the molecules in our study was determined by their different configurations of HOMO orbitals. We present

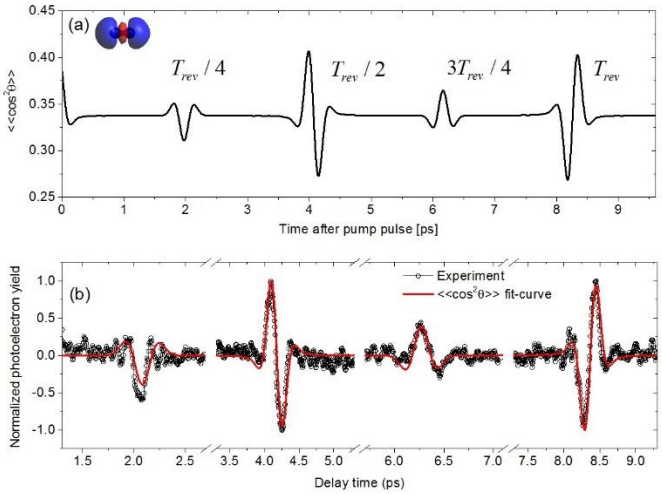


**Figure 2.** (a) The calculated time dependence of the molecular alignment parameter induced by the pump pulse in $N_2$; the configuration of the HOMO is also shown; (b) the time evolution of the measured SFI signal for $N_2$ molecules and the fit curve. Collinearly polarized pump and probe pulses were used with peak intensities of $2\text{x}10^{13}$ W/cm$^2$ and $7.8\text{x}10^{13}$ W/cm$^2$, respectively.

observed temporal signatures of the alignment and compare them to the calculated time evolution of the alignment parameter $\left\langle\left\langle \cos^2\theta \right\rangle\right\rangle$, which depends on the temperature, molecular properties and laser parameters. To demonstrate the effect of the HOMO configuration we present the results for $N_2$ and $C_2H_2$.

Figure 2(a) shows the calculated alignment parameter $\left\langle\left\langle \cos^2\theta \right\rangle\right\rangle$ at temperature T=300 K with our laser parameters and the properties of $N_2$ molecules with rotational constant B=1.9896cm$^{-1}$ [30, 31]. Figure 2(b) depicts the measured signal of the SFI yield for $N_2$ molecules aligned by a linearly polarized pump pulse. The photoelectron yield is smaller at $T_{rev}/4$ and $3T_{rev}/4$ and larger at $T_{rev}/2$ and $T_{rev}$. For the interpretation of the results, we consider the total wave function of a linear molecule, which according to the Born-Oppenheimer approximation can be factorized, $\Psi_{tot} = \psi_{el} \times \psi_{vib} \times \psi_{rot} \times \psi_{ns}$, as a product of the electronic wave function $\psi_{el}$, the vibrational wave function $\psi_{vib}$, the rotational wave function $\psi_{rot}$, and the nuclear spin wave function $\psi_{ns}$. The observed alignment signatures can be explained in the following way. $^{14}N_2$ is a boson, and therefore the total wave function $\Psi_{tot}$ is symmetric [32]. At room temperatures, the electronic $\psi_{el}$ ($^3\sum_g^+$), and the vibrational $\psi_{vib}$ wave functions of $^{14}$N correspond to the ground state, and both are symmetric [32]. Therefore, to understand the $\psi_{rot}$ behavior, we should consider the symmetric and antisymmetric forms of the nuclear spin wave function $\psi_{ns}$ of $^{14}N_2$. For $\Psi_{tot}$ to be symmetric, both $\psi_{rot}$ and $\psi_{ns}$ must be symmetric or antisymmetric. For $^{14}$N the nuclear spin is $I$=1 and the nuclear spin of a $N_2$ molecule takes only values $I_{tot}$=0, 1, or 2. Consequently, $N_2$ exists in even ($I_{tot}$=0, 2) and odd ($I_{tot}$ =1) forms. A state degeneracy with $I_{tot}$ is 2 $I_{tot}$ +1, so the even-$N_2$ and odd-$N_2$ statistical weights are 6 and 3, respectively. Due to the relative abundance of the even-$N_2$ versus odd-$N_2$, 2:1 for even/odd states, their opposed contributions to the $T_{rev}/4$ revival do not cancel completely, however the signal has a reduced amplitude compared to the $T_{rev}$ and $T_{rev}/2$ revivals, as is observed in the experiment (Fig. 2(b)). Consequently, the measured yield in Fig. 2(b) varies in phase with the time dependence of the molecular alignment parameter of Fig 2(a). In Fig. 2(b) we also presented the corresponding fit curve based on Eq. (3) for the alignment parameter $\left\langle\left\langle \cos^2\theta \right\rangle\right\rangle$. Thus we can conclude that the phase shift $\Delta = 0$ for the $N_2$.

The molecular ionization rate is therefore maximal when molecules are aligned along the laser polarization direction and the configuration of the HOMO orbital is parallel to the molecular axis, because such configuration makes ejection of an electron easier. This agrees with the $\sigma_g$ HOMO symmetry of the neutral nitrogen molecule [33], where the molecular ionization rate is maximal, when

the molecules are aligned along the probe polarization direction. As seen in the inset of Fig. 2(a), $N_2$ has its maximum electron density along the internuclear (molecular) axis in its $\sigma_g$ HOMO configuration. By fitting the curve within one full revival period and taking the same laser parameters as experimental ones, we also found the characteristic rotational constant and the corresponding revival time for nitrogen gas. We note that no offset for the time-axis was introduced. The theoretical values of the rotational

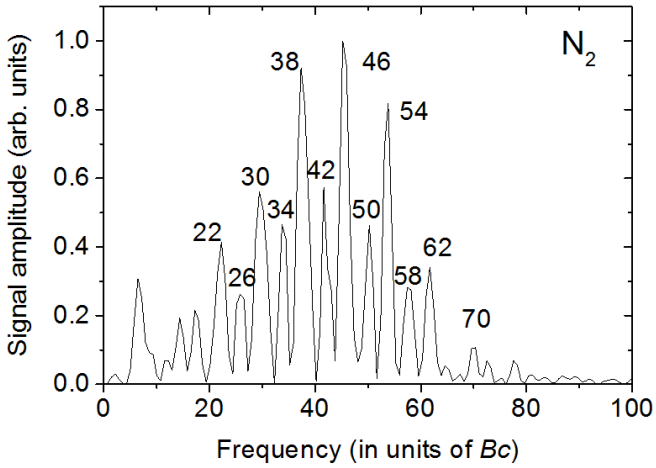


**Figure 3.** Frequency spectrum amplitudes of the measured time-dependent SFI yield for $N_2$ shown in Fig. 2(b). The numbers on spectral peaks, which correspond to the allowed transitions, show the frequencies in terms of $4J$+6. The series (6, 14, 22, 30, 38, 46, 54, …)$Bc$ and (10, 18, 26, 34, 42, 50, 58, …)$Bc$ come from even and odd values of $J$'s, respectively.

constant 1.9896cm$^{-1}$ [30, 31] and the revival time 8.383ps agree well with the experimental values of the rotational constant B=(1.999±0.009)cm$^{-1}$ and the corresponding revival time 8.342ps.

In Fig. 3, we show the corresponding frequency spectrum amplitudes of the measured time-dependent SFI yield for $N_2$ obtained by a Fourier transform (FT) analysis. The spectrum reveals two sequences of allowed Raman transitions obtained from the matrix elements of $\langle\langle\cos^2\theta\rangle\rangle$, which are calculated as $(E_{J+2}-E_J)=(4J+6)hBc$ with the selection rule $\Delta J$=±2. Namely, these sequences are: (6, 14, 22, 30, 38, …)$hBc$ for even $J$'s and (10, 18, 26, 34, 42,…) $hBc$ for odd $J$'s. Recall that the nuclear spin of the nitrogen nucleus is 1, and both even and odd rotational states are permitted for the nitrogen molecule [5]. The relative ratio of the even and odd $J$ states is 2:1, which follows from the nuclear spin statistics and gives an additional factor of ~2 for even $J$'s in the spectrum [34].

Figure 4 (a) shows the alignment parameter $\langle\langle\cos^2\theta\rangle\rangle$ calculated for a temperature T=300 K with our laser parameters for acetylene ($C_2H_2$) molecules with the rotational constant B=1.1766 cm$^{-1}$ [35] and measured time trace of the ionization yield with variations due to alignment of $C_2H_2$ molecules. Acetylene has both even and odd $J$-states, which are populated with the ratio 1:3 [36]. As a result of this fact, even and odd wave packets partially cancel each other, and some alignment and antialignment are observed at quarter revivals as seen in Fig. 4(a,b). The experimental results on molecular revivals of $C_2H_2$ molecules at quarter revival, half revival, three-quarter revival, and full revival are in good agreement with the calculated time dependence of molecular alignment $\langle\langle\cos^2\theta\rangle\rangle$ parameter, but with the inverted polarity. This can be understood from the configuration of HOMO for acetylene, which is dominated by a $\pi_u$ orbital [37]. Molecular orbitals of $\pi_u$ type have higher electron density above/below the internuclear axis, with a node along the internuclear axis, as shown in the inset of Fig. 4(a). Consequently, the temporal structure of $C_2H_2$ revivals in Fig. 4(b) has inverted polarity as compared to the calculated molecular alignment parameter $\langle\langle\cos^2\theta\rangle\rangle$ in Fig. 4(a). With $\Delta=\pi$ the temporal signature of the molecular alignment parameter $\langle\langle\cos^2\theta\rangle\rangle$ is inverted, as seen in Fig. 4 (b), and the calculated function gives the shape similar to the experimental one. The theoretical value of the

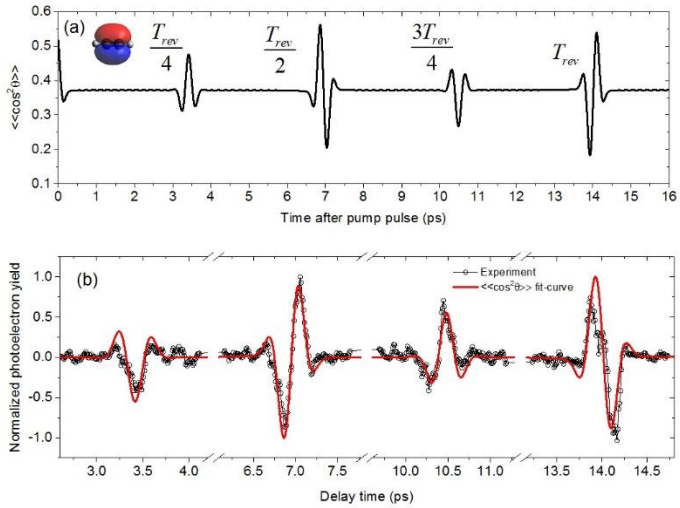


**Figure 4.** (a) The calculated for $C_2H_2$ time dependence of the molecular alignment parameter; the configuration of the HOMO is also shown. (b) The time evolution of the measured SFI signal for $C_2H_2$ and the fit curve. We used linearly polarized pump and probe pulses with peak intensities of $3x10^{13}$ W/cm$^2$ and $7.6x10^{13}$ W/cm$^2$, respectively.

molecular constant for $C_2H_2$, B=1.1766cm$^{-1}$ [35], and the respective revival time 14.175ps match well the characteristic rotational constant B=(1.180±0.003) cm$^{-1}$ and the revival period 14.133ps following from the fitting procedure.

The frequency spectrum of the time-dependent ionization yield for $C_2H_2$ is shown in Fig. 5. The number on each spectral peak shows the frequency in terms of 4*J*+6 which corresponds to allowed Raman transitions, given by the series (6, 14, 22, 30, 38, 46, 54, …)*hBc* for even *J* and by the series (10, 18, 26, 34, 42, 50, 58, …)*hBc* for odd *J*. The relative ratio of the amplitudes of the even and odd spectral components is close to 1:3, following from the nuclear spin statistics.

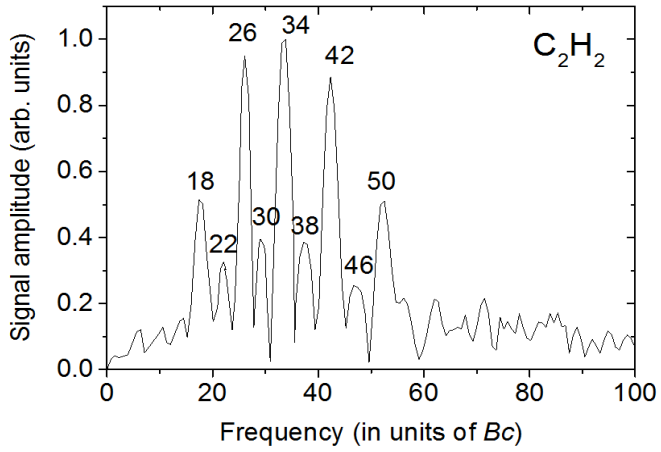


**Figure 5.** Frequency spectrum amplitudes of the measured time-dependent photoelectron yield for $C_2H_2$, shown in Fig. 4(b). The numbers on the spectral peaks show frequencies in terms of 4J+6, which correspond to allowed Raman transitions from the series (6, 14, 22, 30, 38, 46, 54, …)*hBc* for even J and the series (10, 18, 26, 34, 42, 50, 58, …)*hBc* for odd J. The relative ratio of the magnitudes of the spectral harmonics corresponding to even and odd J correlates with the nuclear spin statistics ratio 1:3.

## 5. Impulsive molecular alignment by circularly polarized laser pulses

A combination of a polarizer and a quarter-wave plate placed into the pump arm (Fig. 1) assured the proper circular polarization and power of the pump pulse. A pump pulse with circular polarization produces a net alignment along the laser pulse propagation axis at certain phases of the evolution. This gives the possibility to control alignment of linear molecules outside the plane of polarization, which can provide new capabilities for molecular imaging. As an example we show results for CO, which contains nonidentical nuclei, and therefore no additional factor arises from the nuclear spin statistics [38-40]. Thus, the revivals at odd multiples of $T_{rev}$ / 4 are completely cancelled, whereas only the

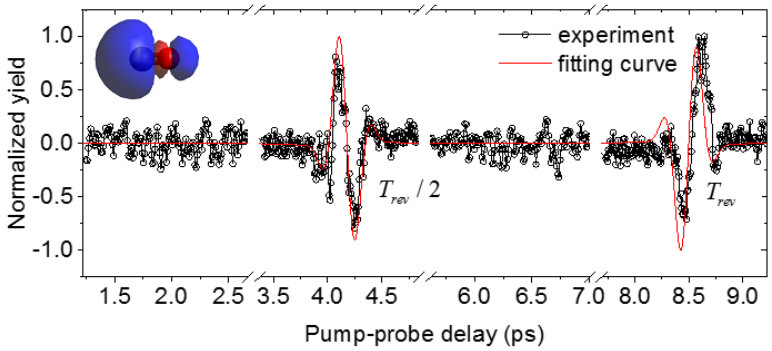


**Figure 6.** Strong-field ionization yield of impulsively aligned CO gas molecules along with the fitting curve.

revivals at multiples of $T_{rev}/2$ remain, as presented in Fig. 6. From the fitting function, we found $\Delta = 0$ for CO, which is similar to the $N_2$ measurements. CO has $\sigma$ HOMOs, so there is no nodal plane along the internuclear axis, and therefore the calculated time dependency of molecular alignment is in phase with the measured strong-field photoelectron yield. For CO, we calculated the characteristic rotational constant as 1.9553cm$^{-1}$, and the corresponding revival period is 8.529ps.

**6. Alignment with arbitrary relative polarizations of pump and probe pulses**

In order to investigate how the structure of the rotational full revival changes with polarization angle α, we ran the experiment for a series of pump-probe delay scans with different linear polarization angles of the pump pulse with respect to the horizontally polarized probe pulse. For this experiment we used a cell filled with $N_2$ gas at typical pressure of 4bar. The created alignment was monitored by the nonlinear spectral modulation of the probe pulse. By blocking the probe pulse, we checked that no spectral modification was produced with the pump pulse only. The resulting structure of such a mapping of the rotational wave packet the so-called "quantum carpet" [22] is shown in Fig. 7: experimental results in

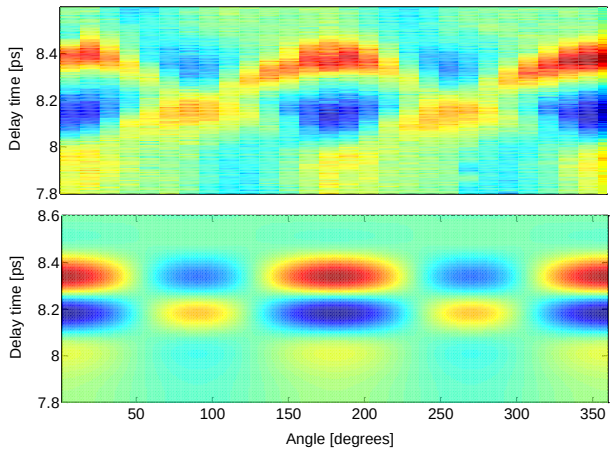


**Figure 7.** Experimental (top) and theoretical (bottom) quantum carpets of a rotational full revival around 8.3ps.

the top and the theoretical calculation in the bottom. The calculation is performed based on Eq. (3) using the relation: $\left\langle\left\langle \cos^2\theta' \right\rangle\right\rangle t = \frac{1}{2}\left(3\cos^2\alpha - 1\right)\left\langle\left\langle \cos^2\theta \right\rangle\right\rangle t + \frac{1}{2}\sin^2\alpha$, where $\theta'$ is the angle between molecular axis and polarization of the probe beam, $\theta$ is the angle between the molecular axis and the field propagation direction of the aligning pulse and $\alpha$ is the relative angle between the polarizations of pump and probe pulses. The angle and delay dependent modulation (Fig. 7) shows that the transmitted power of the probe beam closely correlates with the calculated alignment parameter. The enhancement

/reduction of the alignment is shown by red/blue colours, respectively. We note the existence of angles $\alpha_c \approx 55°$, 125°, 235°, 305°, where the signal is independent of the time delay, which is a specific signature of the $\sigma_g$ symmetry of the active molecular orbital, characteristic of the nitrogen molecule [41].

## 7. Conclusions

The revival signatures of the linear molecules produced by linearly and circularly polarized femtosecond pump pulses have been studied under nonadiabatic alignment conditions and measured by the detection of the strong field ionization photoelectron yield in a pump-probe setup with a variable delay. The revivals at odd multiples of $T_{rev}/4$ are strongly affected by the nuclear spin-statistics factors. The effect of the configuration of the HOMO electron density distribution on the shape of the temporal dependence of the photoelectron yields measured with aligned molecules was discussed. $N_2$ and CO have their maximum electron densities along the internuclear (molecular) axis due to $\sigma_g$ and $\sigma$ HOMOs, respectively. The molecular ionization rate is maximal when molecules are aligned along the laser polarization direction, because such configuration makes ejection of an electron easier. Consequently, in case of $N_2$ and CO our measured photoelectron yields were modulated in phase with the time dependency of the molecular alignment parameter. For the $C_2H_2$, due to the $\pi_u$ HOMO symmetry of $C_2H_2$, which has higher electron density above/below the internuclear axis with a node along the direction of this axis, our experimental photoelectron yields have a polarity-inverted dependence compared to the molecular alignment parameter (a ($-\pi$) shift). By taking into account this additional phase shift a good agreement between calculated and measured alignment signatures was obtained. In addition, the spectra of revivals reveal peaks corresponding to sequences of transitions between even and odd rotational states with amplitude ratios in agreement with the population ratio following from the nuclear spin statistics. Thus, we have demonstrated that the implemented alignment monitoring by measuring photoelectron yields presents a viable and efficient way of studying rotational molecular dynamics. The impulsive alignment of CO molecules with circularly polarized pump pulses was demonstrated. The ability of controlling the alignment of linear molecules outside the plane of polarization can open new capabilities for molecular imaging.

Using an $N_2$-filled gas cell at relatively high pressure (~4bar) we carried out an experiment to study the molecular alignment wakes of femtosecond laser pulses by modulation of the probe pulse. The variations of the transmitted probe pulse were explained by the induced intensity-dependent variations of the nonlinear absorption. In addition, we mapped ultrafast rotational wave packets as a function of the pump-probe delay and the angle between their polarizations (i.e. a "quantum carpet" was experimentally measured).

## Acknowledgments

This work was supported by the Robert A. Welch Foundation Grant No. A1546, and the Qatar Foundation under the grant NPRP 6-465-1-091.

## References

[1] Xu N, Li J, Li J, Zhang Z and Fan Q 2011 *Lasers - Applications in Science and Industry*, ed K. Jakubczak, p 229
[2] Stapelfeldt H and T Seideman T 2003 *Rev. Mod. Phys.* **75** 543
[3] Seideman T and Hamilton E 2005 *Adv. At., Mol., Opt. Phys.* ed P R Berman and C C Lin (Cambridge: Academic Press) **52** 289
[4] Henrik S 2004 *Phys. Scr.* **2004** 132.
[5] Fleischer S, Averbukh I S and Prior Y 2006 *Phys. Rev.* A **74** 041403
[6] Itatani J, Levesque J, Zeidler D, Niikura H, Pepin H, Kieffer J C , Corkum P B and Villeneuve D M 2004 *Nature* **432** 867
[7] Gordon R J, Zhu L, Schroeder W A and Seideman T 2003 *J. Appl. Phys.* **94** 669
[8] Bartels R A, Weinacht T C, Wagner N, Baertschy M, Greene C H, Murnane M M and Kapteyn H C 2001 *Phys. Rev. Lett.* **88** 013903 (2001).

[9] Lee K F, Villeneuve D M, Corkum P B and Shapiro E A, 2004 *Phys. Rev. Lett.* **93**, 233601
[10] Zewail A H 2000 *J. Phys. Chem.* A **104**, 5660
[11] Pavičić D, Lee K F, Rayner D M, Corkum P B and Villeneuve D M 2007 *Phys. Rev. Lett.* **98**, 243001

[12] Péronne E, Poulsen M D, Bisgaard C Z, Stapelfeldt H and Seideman T 2003 *Phys. Rev. Lett.* **91**, 043003
[13] Nevo I, Holmegaard L, Nielsen J H, Hansen J L, Stapelfeldt H, Filsinger F, Meijer G and Kupper J 2009 *Phys. Chem. Chem. Phys.* **11** 9912
[14] Vozzi C, Calegari F, Benedetti E, Caumes J P, Sansone G, Stagira S, Nisoli M, Torres R., Heesel E, Kajumba N, Marangos J P, Altucci C and Velotta R 2005 *Phys. Rev. Lett.* **95** 153902
[15] Ripoche J-F, Grillon G, Prade B, Franco M, Nibbering E, Lange R and Mysyrowicz A 1997 *Opt. Commun.* **135** 310
[16] Calegari F, Vozzi C, Gasilov S, Benedetti E, Sansone G, Nisoli M, De Silvestri S.and Stagira S 2008 *Phys. Rev. Lett.* **100** 123006 (2008).
[17] Kaya N, Kaya G, Sayrac M, Boran Y, Anumula S, J. Strohaber, A. A. Kolomenskii and H. A. Schuessler, *Opt. Express* **24** 2562 (2016).
[18] Smeenk C T L, Arissian L, Sokolov A V, Spanner M, Lee K F, Staudte A, Villeneuve D M and Corkum P B 2014 *Phys. Rev. Lett.* **112** 253001
[19] Smeenk C T L and Corkum P B 2013 *J. Phys. B At. Mol. Opt. Phys.* **46** 201001
[20] Couairon A and Mysyrowicz A 2007 *Phys. Rep.* **441** 47
[21] Chen Y H , Varma S and Milchberg H M 2008 J. Opt. Soc. Am. B **25** B122
[22] Bryan W A, English E M L, McKenna J, Wood J, Calvert C R, Turcu I C E, Torres R, Collier J L , Williams I D and Newell W R 2007 *Phys. Rev.* A **76**, 023414
[23] Seideman T 1997 *J. Chem. Phys*. **107** 10420
[24] Graybeal J D *Molecular Spectroscopy* 1988 (McGraw-Hill: New York)
[25] Purcell S M and Barker P F 2010 *Phys. Rev. A* **82** 033433
[26] Purcell S M Barker P F 2009 *Phys. Rev. Lett.* **103** 153001
[27] Ortigoso J, Rodríguez M, Gupta M and Friedrich B 1999 *J. Chem. Phys*. **110** 3870.
[28] Yuan S, Li M, Feng Y, Li H, Zheng L, Chin S L and Zeng H, *J. Phys. B At. Mol. Opt. Phys.* **48**, 094018 (2015)
[29] Kaya G, Kaya N, Strohaber J, Hart N A, Kolomenskii A A and Schuessler H A *Appl. Phys.* B **122** 288 (2016)
[30] Haynes W M L D R 2011*CRC handbook of chemistry and physics: a ready-reference book of chemical and physical data* (Boca Raton: CRC Press)
[31] Bendtsen J 1974 *J. Raman Spectrosc.* **2** 133-45.
[32] Atkins P, de Paula J and Friedman R 2009 *Quanta, Matter, and Change: A Molecular Approach to Physical Chemistry* (Oxford: Oxford University Press)
[33] Tong X M , Zhao Z X and Lin C D 2002 *Phys. Rev.* A **66** 033402
[34] Faisal F H M, Abdurrouf A , Miyazaki K and Miyaji G 2007 *Phys. Rev. Lett.* **98** 143001
[35] Herman M, Campargue A, El Idrissi M I and Vander Auwera J 2003 J. *Phys. Chem. Ref. Data* **32**, 921
[36] Li H, Li W, Feng Y, Liu J, Pan H and Zeng H 2012 *Phys. Rev.* A **85** 052515
[37] Torres R, Kajumba N, Underwood J G, Robinson J S, Baker S, Tisch J W G, de Nalda R, Bryan W A, Velotta R, Altucci C, Turcu I C E and Marangos J P 2007 *Phys. Rev. Lett*. **98** 203007
[38] R B Philip and Per J 2006 *Molecular Symmetry and Spectroscopy, 2nd Ed* (Ottawa: NRC Research Press)
[39] McQuarrie, D A and J D Simon 1997 *Physical Chemistry: A Molecular Approach* (Herndon: University Science Books)
[40] Kaya N, Kaya G, Strohaber J, Kolomenskii A A and Schuessler H A 2016 *Eur. Phys. J.* D **70** 224
[41] Abdurrouf A and Faisal F H M 2009 *Phys. Rev.* A **79** 023405